NASA TECHNICAL NOTE

NASA TN D-6868

c.1

NASA TN D-6868

MASS INFLUX OBTAINED FROM LLLTV OBSERVATIONS OF FAINT METEORS

by Robert J. Naumann and K. Stuart Clifton

George C. Marshall Space Flight Center
Marshall Space Flight Center, Ala. 35812

NATIONAL AERONAUTICS AND SPACE ADMINISTRATION • WASHINGTON, D. C. • JULY 1972

1. Report No. NASA TN D-6868	2. Government Accession No.	3. Recipient's Catalog No.
4. Title and Subtitle: Mass Influx Obtained From LLLTV Observations of Faint Meteors*		5. Report Date: July 1972
		6. Performing Organization Code
7. Author(s): Robert J. Naumann and K. Stuart Clifton		8. Performing Organization Report No.: M445
9. Performing Organization Name and Address: George C. Marshall Space Flight Center, Marshall Space Flight Center, Alabama 35812		10. Work Unit No.: 124-09-23-0000
		11. Contract or Grant No.
12. Sponsoring Agency Name and Address: National Aeronautics and Space Administration, Washington, D.C. 20546		13. Type of Report and Period Covered: Technical Note
		14. Sponsoring Agency Code

15. Supplementary Notes
Prepared by Space Sciences Laboratory, Science and Engineering

*Presented at I.A.U. Colloquium #13, "The Evolutionary and Physical Problems of Meteoroids," Dudley Observatory, Albany, New York

16. Abstract

Since the advent of low light level television (LLLTV) systems, it has been recognized that such devices offer the ability to observe meteors as faint as 10th magnitude which allows the extension of optical meteor data to masses as small as 10^{-4} gram. The Space Sciences Lab at Marshall Space Flight Center has been actively engaged in such observations using image orthicons and intensified SEC vidicons.

The results of these observations are presented along with an interpretation in terms of mass-flux. This interpretation includes the development of a relationship between peak luminosity of a meteor and mass, velocity, and zenith angle that was derived from single body meteor theory and compares favorably with results obtained from the Artificial Meteor Program. Also included in the mass flux interpretation is an analysis of the observation response of a LLLTV system to fixed and moving point sources.

17. Key Words (Suggested by Author(s))	18. Distribution Statement

19. Security Classif. (of this report)	20. Security Classif. (of this page)	21. No. of Pages	22. Price*
Unclassified	Unclassified	23	$ 3.00

* For sale by the National Technical Information Service, Springfield, Virginia 22151

TABLE OF CONTENTS

LIST OF ILLUSTRATIONS

MASS INFLUX OBTAINED FROM LLLTV OBSERVATIONS OF FAINT METEORS

INTRODUCTION

The present model of the meteoroid mass distribution is based on an extrapolation from ground based photographic observations of the larger meteoroids with masses of the order of grams to satellite-borne penetration measurements of meteoroids with masses in the microgram range. The mass range representing the greatest damage potential to manned space vehicles is from 1 to 100 milligrams. The fact that the meteoroid population in this region must be inferred from an extrapolation over 6 orders of magnitude between two points that are determined by completely different properties of meteoroids through interactions that are poorly understood physically and cannot be adequately tested experimentally, has caused some concern among those responsible for establishing the meteoroid environment. Also, there are legitimate scientific reasons for extending the ground based optical measurements to fainter meteors. Of primary interest is the determination of the slope of the mass distribution curve or the population index parameter. This will greatly improve the confidence in the extrapolation as well as reduce the range over which the extrapolation must be carried out, and will provide a badly needed consistency check between the ground-based and satellite measurements.

This paper discusses the techniques and results of using LLLTV observations to determine the meteoroid mass distribution in the region from grams to milligrams.

DESCRIPTION OF THE SYSTEM

Recent developments in low-light-level television (LLLTV) systems have allowed the observation of much fainter meteors than could be photographed. This improvement results primarily from the much higher quantum efficiency of the photodetector which results in much smaller integration times. This is particularly important in meteor work since it is advantageous to have the integration time shorter than the event duration. Our system consists of a Commercial Electronics camera chain using a Westinghouse WL-32000 Intensifier-SEC vidicon tube with a 105 mm f/.75 Rayxar lens. This affords a 13° by 16° field of view. The effective integration time of the system is very close to the standard frame time of 1/30 sec, which is ideal for meteor work.

The ultimate theoretical sensitivity for the system is $m_v = 14.26$. This was estimated by requiring a star to produce 1 photoelectron at the photocathode per integration time. The system is invariably limited by sky background which, even under ideal conditions, is 2 orders of magnitude above dark current. Stars as faint as $m_v = 11$ have been observed which is close to the theoretical limit of 11.6 for a sky background of 300 $m_v = 10$ stars/deg^2, and a S/N = 5.

For moving objects such as meteors, this limiting magnitude would apply to meteors moving nearly parallel to the optical axis so that they would remain within a resolving element for one integration time. For most meteors, the S/N will be decreased because the time they contribute to a resolving element is limited by the writing speed of their image. It is estimated that if the system has an observing limit of 11 magnitude for stars, it will see all meteors brighter than $m_v = 6.4$ and 50 percent of the meteors brighter than $m_v = 8.15$.

ANALYSIS PROCEDURES

Even though the dynamic range of a TV image is limited, photometry of point images can still be performed over as much as 6 orders of magnitude by making use of the fact that the image spreads after it reaches saturation [1]. Thus, the amount of light associated with the image is a monotonic, if not linear, function of input. The difficulty lies in the fact that obtaining light curves from the TV monitor is a time consuming and laborious task, especially for the faint meteors. Until the special video processing systems presently being developed for this purpose are available, it will not be possible to obtain light curves on a sufficient sample of meteors to establish a good distribution.

An alternative procedure, which is less time consuming, was adopted for interim use. This consists of treating the video system as a threshold detector and simply counting those meteors that are above the detection threshold. By varying the threshold through reduction of the lens aperture setting, a cumulative distribution in peak meteor magnitude is obtained.

Figure 1 shows the results of this mode of operation during two observing periods at Climax, Colorado. The camera was oriented toward the zenith.

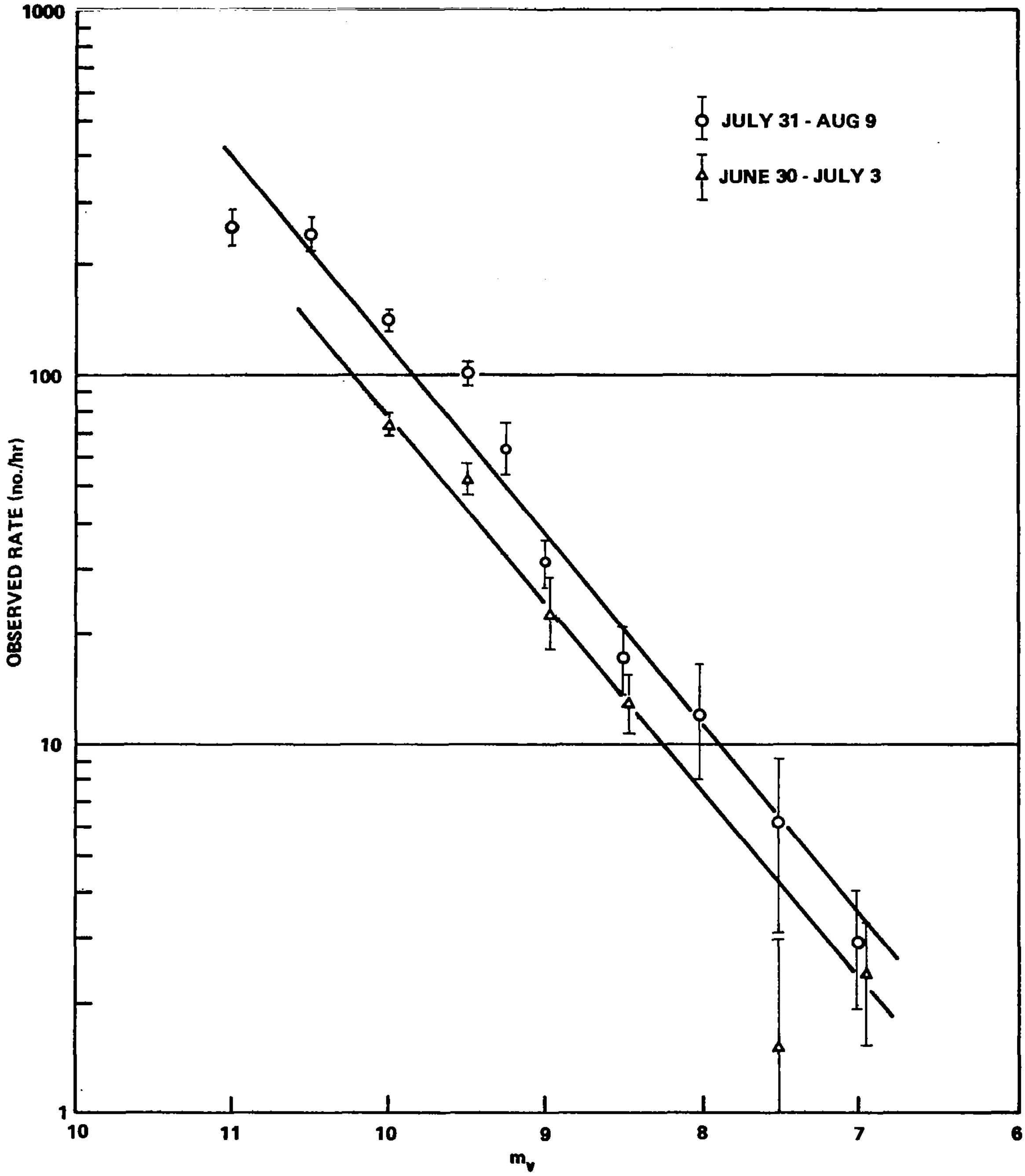

Figure 1. Observed meteor rates as a function of limiting magnitude. (Error bars represent 1 σ limits based on the statistical sample.)

Care was taken to program the aperture settings to assure a uniform distribution of observing time at each aperture setting throughout the night. The higher rates in the period from July 31 through August 9 may be attributed to the presence of the Perseids and the δ - Aquarids during this period. The details of these data will be published separately.

Taking the area of the sky within the field of view to be 640 km^2 the observed rates for the non-shower period can be expressed

$$\log \phi = -15.482 + 0.5008 \, m_v \tag{1}$$

where ϕ is the observed rate of meteors (number/m^2/sec) when m_v is the limiting magnitude. This limiting magnitude is taken to be the magnitude of the faintest AO star detectable on the video screen. In a sense, this limiting magnitude represents the faintest meteor that could be detected, although practically all detectable meteors will be brighter than this because of their writing speed.

RELATIONSHIP BETWEEN PEAK LUMINOSITY AND METEOR MASS

A statistical analysis by Jacchia, Verniani, and Biggs [2] of the peak brightness of meteors in terms of their mass, velocity, and entry angle yielded the result

$$I_P = 10^{-4.636} \, m_o^{0.9} \, v^{3.5} \, (\cos \theta)^{0.6} \tag{2}$$

where I_P is the peak intensity in units of zero magnitude stars, m_o is the initial meteor mass in grams, v is the entry velocity in km/sec, and θ is the entry angle or the angle between the velocity vector and the zenith.

A similar result can be derived from the classical single body meteor theory by assuming that the rate of mass loss is equal to the energy input divided by the heat of vaporization L. In the free molecular regime

$$\dot{m} = \frac{A \rho v^3}{2L} = - \frac{S m^{2/3} \rho v^3}{2L \rho_m^{2/3}} \tag{3}$$

where S is the shape factor (S = 1.208 for a sphere), ρ_m is the density of the meteoroid, and ρ is the atmospheric density. This neglects radiation losses, which are small compared to the heat input even at the boiling point of Fe (3160° K); and neglects any change in shape factor with time. Neglecting deceleration, which amounts to only a small percent velocity change in the time it takes a small meteoroid to completely burn up, and assuming an exponential atmosphere, equation (3) becomes

$$\dot{m} = -\frac{S m^{2/3} v^3}{2L\rho_m^{2/3}} \rho_H e^{-x/h} \qquad (4)$$

where $x = -vt \cos\theta$, h is the scale height, and ρ_H is the atmospheric density at $x = 0$. This differential equation may be solved by separation of variables. It is convenient to define $t = 0$ at meteor burnout, or $m = 0$. The solution is then

$$m = m_o \left(1 - e^{\beta t}\right)^3 \qquad (5)$$

where

$$\beta = \frac{v \cos\theta}{h}$$

and m_o, the initial mass, is

$$m_o = \left(\frac{S v^3 \rho_H}{6L\rho_m^{2/3}\beta}\right)^3$$

Differentiating the solution,

$$\dot{m} = -3\beta m_o \left(1 - e^{\beta t}\right)^2 e^{\beta t} \quad . \qquad (6)$$

The peak $\dot{m}$ is obtained by equating $\ddot{m}$ from (6) to 0 to find the time t_p when $\dot{m}$ is maximized. This yields

$$e^{\beta t_p} = 1/3 \quad .$$

Putting this in (5),

$$\dot{m}_p = -\frac{4}{9}\beta m_o \quad . \tag{7}$$

The radiant intensity from a meteor is given by

$$I = -\frac{\tau}{2}\dot{m}v^2 \tag{8}$$

where τ is the luminous efficiency. Using equation (7),

$$I_P = \frac{\tau}{2}\,\frac{4}{9}\,\frac{m_o v^3}{h}\cos\theta \quad . \tag{9}$$

The luminous efficiency for Fe has been determined experimentally from Trailblazer [3] and is expressed by $\tau = 10^{-17.95}$ v (cm/sec). Figure 2 compares the light curve obtained with this model with an observed light curve from one of the Fe Trailblazer meteors.

For stony meteors, Cook, Jacchia, and McCrosky [4] recommend

$$\tau = 10^{-18.91}\ v\ (\mathrm{cm/sec}) \tag{10}$$

which is consistent with estimates of Ayers, McCrosky, and Shao based on the Trailblazer measurements.

Putting this value in equation (9), and choosing $h = 5.4$ km, which corresponds to 80 km, results in

$$I_P = 10^{-5.297} m_o v^4 \cos\theta \tag{11}$$

with the units the same as in (2). For the case of a 1-gm meteor at 22 km/sec, typical of cases from which equation (2) was obtained,

$$I_P = \begin{cases} 1.154 & \text{(equation 2)} \\ 1.182 & \text{(equation 11)} \end{cases} \quad .$$

The fact that the simple theory yields almost identical results as the empirical approach, together with the desirability of having some theoretical basis for determining the functional relationship of luminous intensity with mass,

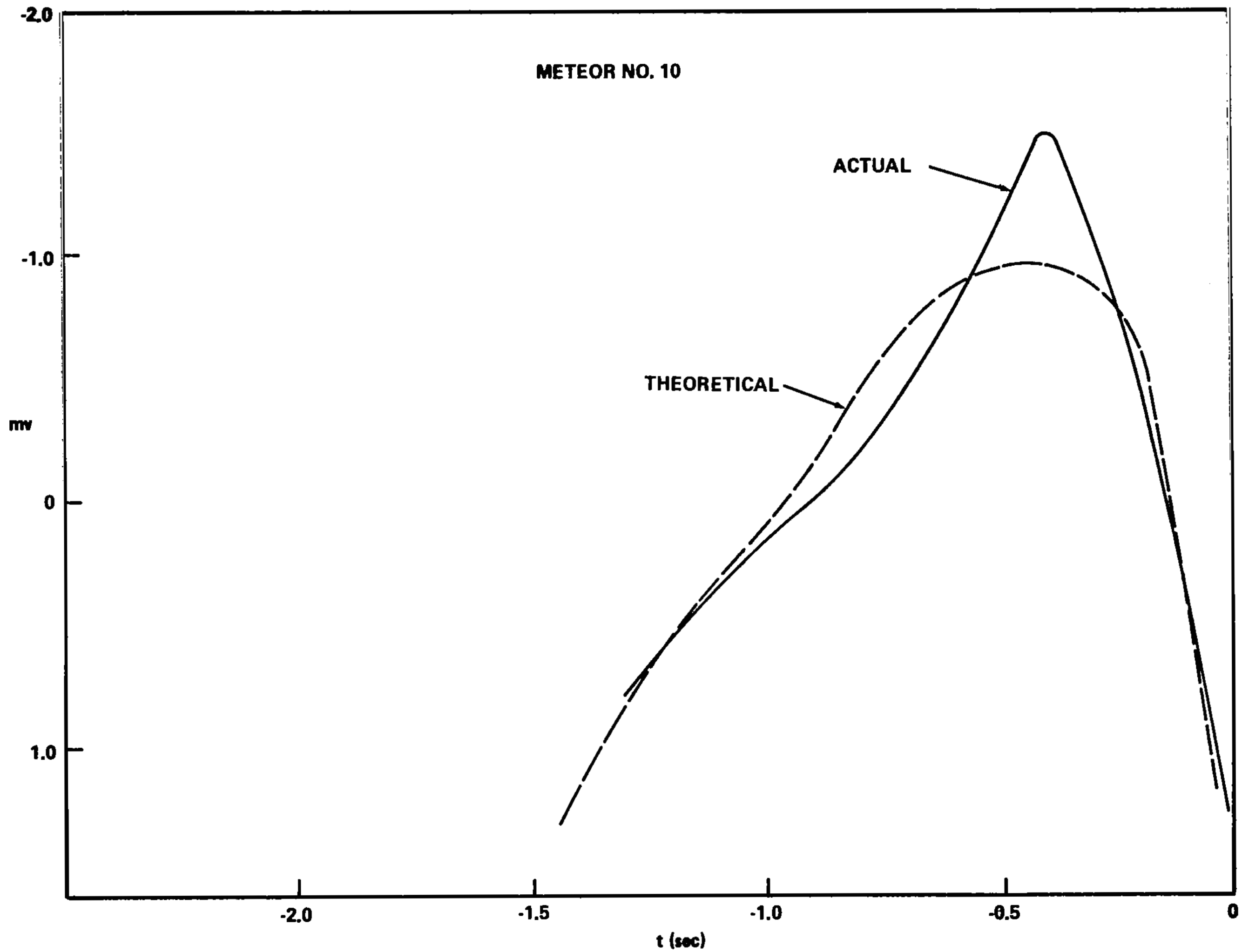

Figure 2. Comparison of theoretical light curve compared with the measured light curve of an artificial meteor.

velocity, and entry angle, are the bases for choosing equation (11) as the functional observing relationship for the analysis.

SYSTEM RESPONSE TO MOVING TARGETS

As was stated previously, the detection threshold of a moving object is increased because the photons are spread over a number of resolving elements instead of contributing to the signal in a single element. A first order attempt to derive the system response to moving targets is to simply require that the minimum detectable moving object deliver the same number of photons during the time it resides in a resolving element as a minimum detectable stationary object in one integration time. The residence time is

$$t = \frac{A_r^{1/2}}{F\omega} \tag{12}$$

where A_r is the area of a resolving element, F is the focal length of the lens, and ω is the angular rate.

The criterion for detectability is

$$I_L \frac{A_r^{1/2}}{F\omega} = I_T \tau \tag{13}$$

where I_T is the threshold intensity for stationary objects, I_L is the limiting intensity for moving objects, and τ is the integration time. The photocathode is 40 mm in diameter, or 24 mm from the top to the bottom raster line. Since there are 525 lines, a resolving element is taken to be a square 24/525 mm per side. Taking $F = 105$ mm and $\tau = 1/30$ sec,

$$I_L = I_T\, 76.57\,\omega\,; \qquad \omega \geq 0.01306 \text{ rad/sec} \tag{14}$$

Figure 3 compares this model of the response to moving point sources with measurements made in our laboratory. The measurements consisted of projecting point sources onto a mirror mounted on a rate table which reflected the

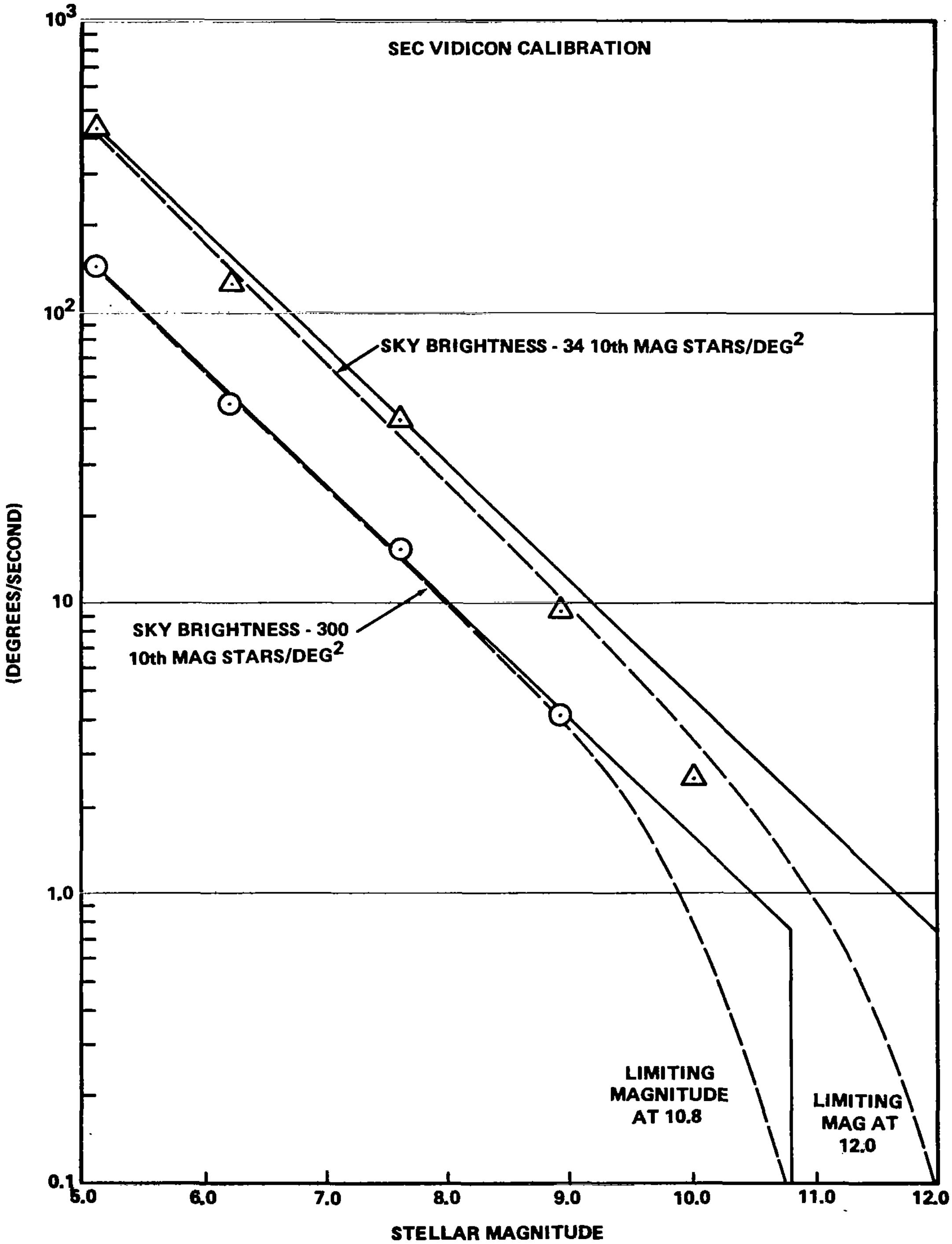

Figure 3. Response of the SEC Vidicon to moving point images. (The solid curves represent the predicted response based on the detection criteria used in the analysis.)

image onto a projection screen. The point source consisted of a precision 50 μ pinhole mounted in a 35 mm slide projector. Neutral density filters were used to vary the image intensity, and the various images were calibrated by a photomultiplier photometer. The background lighting was provided by a small flood lamp with a controllable aperture. The angular rate of the mirror was adjusted for each filter until the image could no longer be detected on the monitor screen.

The agreement between the simple model and the observed results justify the model. The only discrepancy occurs in the transition at the point where the image spends τ in a resolving element. Since the image in the experiment is smaller than the resolving element, but is not an infinitesimal, some rounding off of the theoretical model in this transition region is to be expected, which of course is the observed result.

Since the angular rate

$$\omega = \frac{v \sin\theta}{r} \quad , \tag{15}$$

and using $r = 80$ km typical of meteor heights, equation (15) becomes

$$I_L = \begin{cases} I_T \, 0.957\, v \sin\theta \\ I_T \end{cases} \tag{16}$$

whichever is greater.

RELATION BETWEEN INCIDENT FLUX AND OBSERVED FLUX

The number of meteors observed per unit area time is given by

$$\phi = \int_{\text{hemisphere}} d\Omega \quad \cos\theta \int_0^\infty dv \int_{m_T\left(I_T\, ,\, \theta\, ,\, v\right)}^\infty dm \; n_{mv} \tag{17}$$

where n_{mv} is the directional mass velocity distribution (no. per unit area, time, solid angle with masses between m and m+dm and velocities between v and v+dv). The integration is carried out from the threshold m_T required to produce an observed signal, which is a function of the threshold response of the system I_T, θ, and v. Given only the observed ϕ, clearly there is not sufficient information to solve the integral equation. Several simplifying assumptions are in order. First, to a good approximation the velocity and mass distributions are independent. Second, it will be assumed that the velocities are isotropically distributed; i.e., n_{mv} is independent of θ and ϕ. Equation (17) becomes

$$\phi = 2\pi \int_0^{\pi/2} \cos\theta \ \sin\theta \ d\theta \int_0^\infty n_v \, dv \int_{m_T\left(I_T, \theta, v\right)}^\infty n_m \, dm \quad . \tag{18}$$

Even assuming n_v is known, there is still insufficient information to define n_m. However, the fact that the observed ϕ can be expressed as a power law, equation (1), suggests the cumulative mass flux N_m (no. per unit area time with mass m or greater) can be expressed

$$N_m = \pi \int_{m_T}^\infty N_m \, dm = C \, m_T^{-\alpha}$$

where α is the population index. With this assumption equation (18) becomes

$$\phi = 2C \int_0^{\pi/2} \cos\theta \ \sin\theta \ d\theta \int_0^\infty n_v \, dv \, m_T^{-\alpha}\left(I_T, \theta, v\right) \quad . \tag{19}$$

The threshold mass is from equation (11)

$$m_T = I_L \ 10^{5.297} \ v^{-4} \ (\cos\theta)^{-1}$$

But from equation (16)

$$m_T = \begin{cases} I_T \ 10^{5.297} \ v^{-4} \left(\cos\theta\right)^{-1} & ; \ \theta \geq \theta_o \\ 0.957 \ I_T \ 10^{5.297} \ v^{-3} \tan\theta & ; \ \theta \leq \theta_o \end{cases} \tag{20}$$

where

$$\theta_o = \sin^{-1} \frac{1}{0.957\, v} \quad .$$

Equation (19) becomes

$$\phi = 2C I_T^{-\alpha} \, 10^{-5.297\alpha} \left[\int_0^\infty v^{4\alpha} n_v \, dv \int_0^{\theta_o(v)} (\cos\theta)^{1+\alpha} \sin\theta \, d\theta \right.$$

$$\left. + (0.957)^{-\alpha} \int_0^\infty v^{3\alpha} n_v \, dv \int_{\theta_o(v)}^{\pi/2} (\cos\theta)^{1+\alpha} (\sin\theta)^{1-\alpha} \, d\theta \right] \quad . \qquad (21)$$

It is convenient to introduce an average $\bar{m}$ defined as the mass of a just detectable meteor having average velocity and $\theta = 45°$. From equation (20)

$$\bar{m} = 0.957 \, I_T \, 10^{5.297} \, v^{-3} \tan 45° \quad . \qquad (22)$$

Equation (21) becomes

$$\phi = \frac{2C\bar{m}^{-\alpha}}{v^{3\alpha}} \left[(0.957)^{\alpha} \int_0^\infty v^{4\alpha} n_v \, dv \int_0^{\theta_o(v)} \cos\theta^{1+\alpha} \sin\theta \, d\theta \right.$$

$$\left. + \int_0^\infty v^{3\alpha} n_v \, dv \int_{\theta_o(v)}^{\pi/2} (\cos\theta)^{1+\alpha} (\sin\theta)^{1-\alpha} \, d\theta \right] \quad . \qquad (23)$$

The first integral is the contribution from those meteors moving nearly along the line of sight that remain in a single resolving element for one integration time. Since θ_o is typically 3°, this contribution is small and can be ignored. The integral over θ in the second integral must be evaluated numerically unless α is an integer. The lower limit $\theta_o(v)$ is a function of v, as may be seen in Figure 4. This dependence is not strong for $\alpha \approx 1$. Therefore an average value of $v = 20$ km/sec will be used which yields $\theta_o = 3°$.

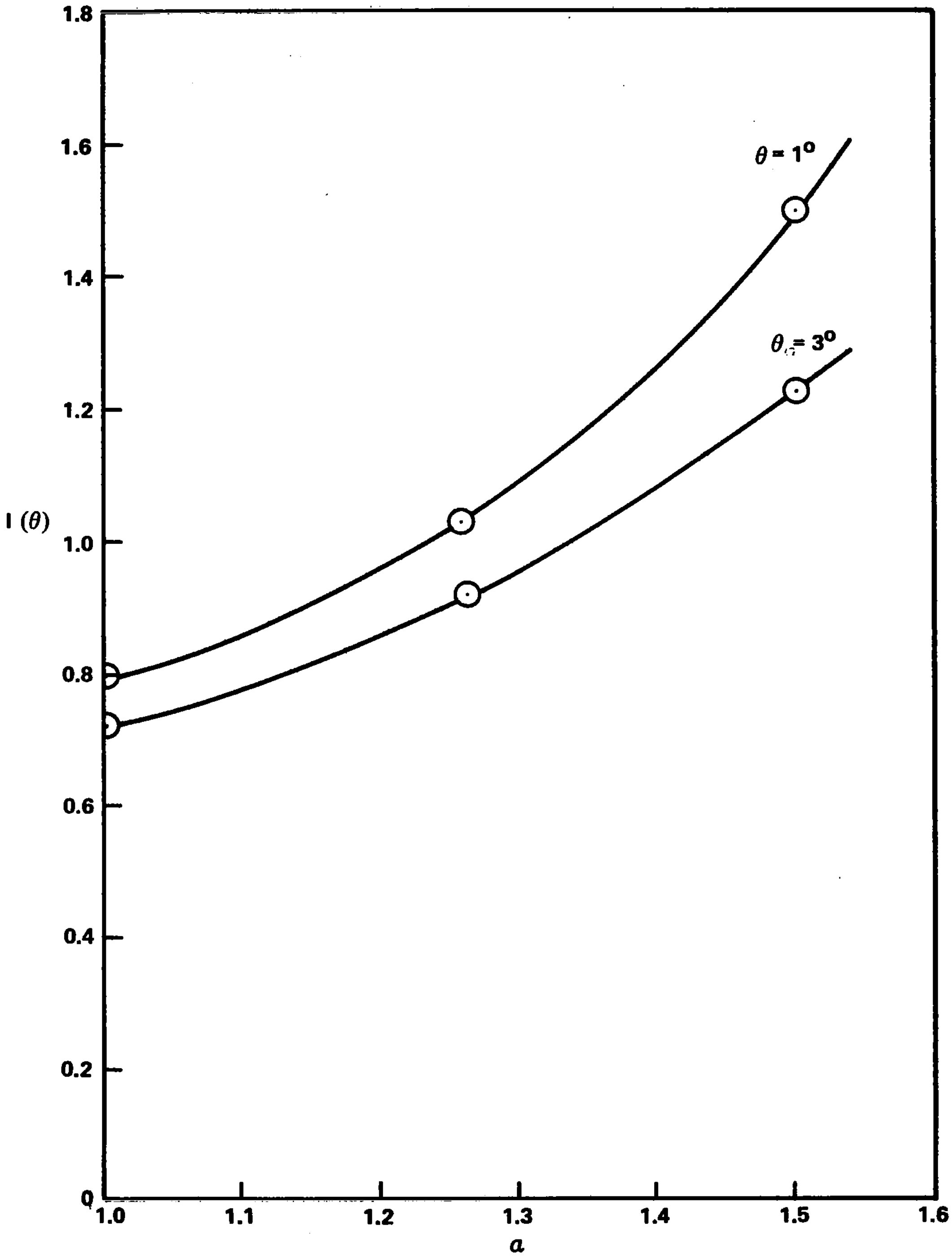

Figure 4. The value of the integral $I(\theta)$ in equation (25) as a function of θ_o and α.

The velocity distribution was adopted from the work of Dohnanyi [5], and expressed as

$$n_v = \begin{cases} C_N \, v^{1.6} & ; \quad 11.2 \le v \le 16.6 \\ C_N \, 1.61 \times 10^7 \, v^{-4.3} & ; \quad 16.6 \le v \le 72.2 \end{cases} \tag{24}$$

The normalization constant is $C_N = 0.001153$. The $\langle v \rangle$ using this distribution is 19.2 km/sec. The weighted average $\langle v^x \rangle / \langle v \rangle^x$ is shown in Figure 5.

Equation (23) can be written

$$\phi = 2 \frac{\langle v^{3\alpha} \rangle}{\langle v \rangle^{3\alpha}} I(\theta) N_{\bar{m}_T} \tag{25}$$

where $N_{\bar{m}_T}$ is the cumulative isotropic mass flux of meteroids having mass $\bar{m}_T$ or greater, $\bar{m}$ is given by equation (22), and $I(\theta)$ is

$$I(\theta) = \int_{\theta_o}^{\pi/2} (\cos\theta)^{1+\alpha} (\sin\theta)^{1-\alpha} \, d\theta \quad .$$

Since $I_T = 10^{-0.4 m_v}$ and the observational results were found to be [equation (1)]

$$\log \phi = -15.352 + 0.5053 \, m_v \quad ,$$

$$\log \phi = -15.352 - \frac{0.5053}{0.4} \log I_T \quad . \tag{26}$$

Differentiating the log of equation (21)

$$\frac{d(\log \phi)}{d(\log I_T)} = -\alpha$$

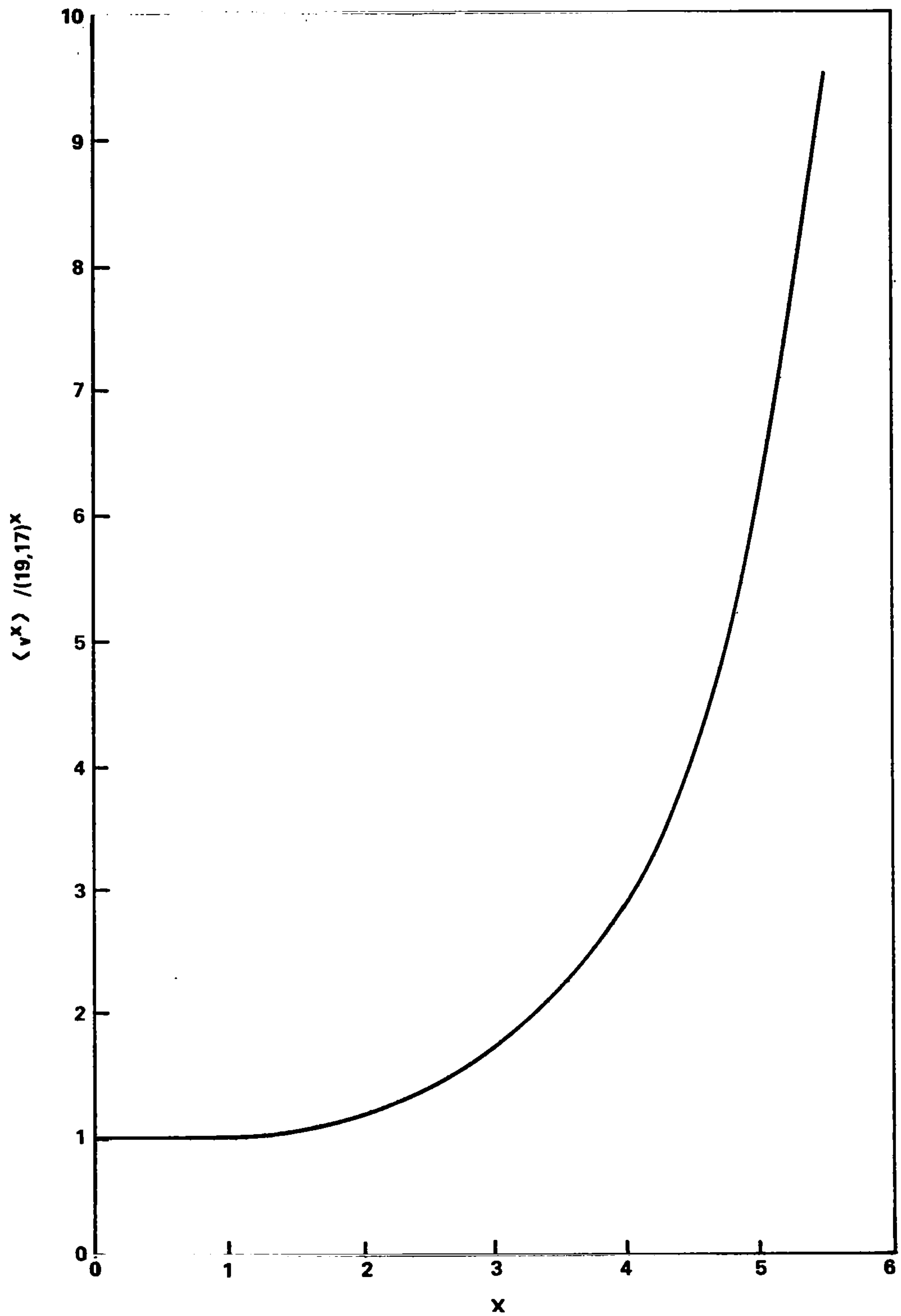

Figure 5. The value of the moments of the velocity distribution computed from Dohnanyi's velocity distribution.

From equation (26) α is found to be 1.263. Using this value in Figures 4 and 5

$$\frac{\langle v^{3.78} \rangle}{\langle v \rangle^{3.78}} = 2.48$$

$$I(\theta) = 0.933$$

Combining equations (22), (25), and (26) results in

$$\log N_{\overline{m}_T} = -15.352 - 1.263 \ (\log \overline{m}_T - 1.466) - \log 2 - \log 2.48 - \log 0.933 \qquad (27)$$

or

$$\log N_{\overline{m}_T} = -14.24 - 1.263 \log \overline{m}_T \quad .$$

The observed range from $m_v = 7$ to $m_v = 10$ corresponds to a mass range of $10^{-1.334}$ to $10^{-2.534}$ gm. The result of equation (27) is compared with the existing distribution of meteors in Figure 6. The result from the July 31 - August 9 expedition is also shown, which contains the Perseids and δ-Aquarids. No attempt was made to alter the distributions in velocity and angle to account for the shower component.

COMPARISON WITH OTHER DATA

Figure 6 shows the relationship of the data obtained in this work with the current meteoroid mass distribution adopted by NASA [6]. Also shown for comparison is the Hawkins and Upton datum point [7] based on photographic meteors, and the points obtained from the Pegasus [8] and Explorer XXIII [9] penetration experiments. These data have been analyzed in terms of encounter frequency, i.e., number incident per unit area time on a surface without regard to angle of incidence of velocity. The NASA design curve refers to the number capable of penetrating a surface per unit area time, which can just be penetrated by a meteoroid with the specified mass under conditions of normal impact at the average velocity (assumed to be 20 km/sec) and average density (assumed to be 0.5 gm/cm^3). Integrating over the velocity and angular

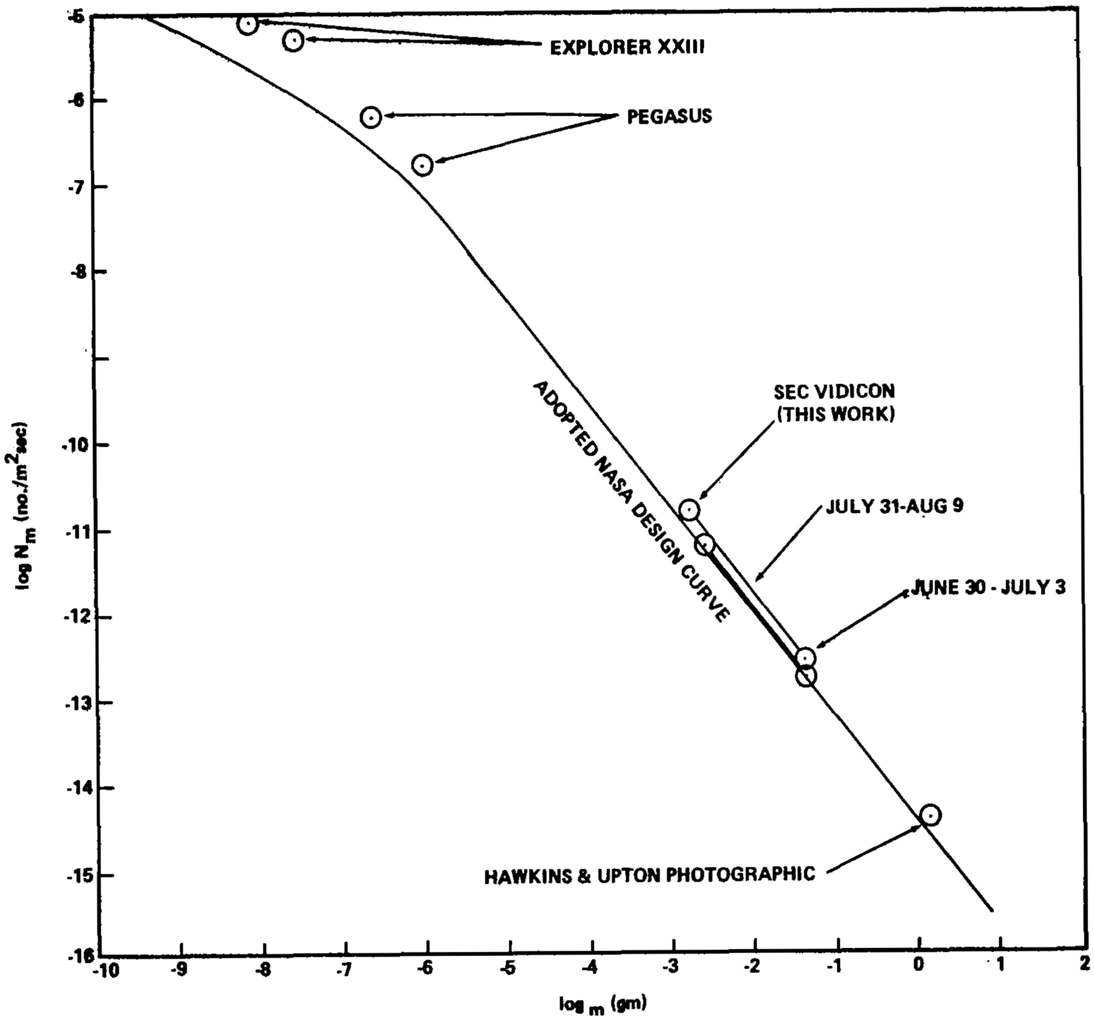

Figure 6. Comparison of the results of this study with other work and with the adopted NASA meteoroid environmental design criteria. (The observed data represent encounter frequency, whereas the design criteria is weighted to express penetration frequency.)

distributions weighted appropriately for penetration mechanics results in the penetration frequency being less than the encounter frequency by a factor of approximately 2 [10].

The penetration data from Pegasus and Explorer XXIII were analyzed using recent calibration data [11]. The discrepancy between these data points and the NASA model is partially due to the difference between encounter frequency and penetration frequency, but also includes the departure from linear size scaling in thin metallic targets. Again, the design curve was derived from the actual penetration data using the conventional penetration formula, and will serve adequately as a design criteria so long as the same formula is used to convert back to penetration results. However, this departure should be considered in developing a true mass distribution.

CONCLUSIONS

A technique has been developed, using the SEC vidicon LLLTV system as a threshold detector for faint meteors, to obtain mass flux distribution data in the mass range from 1 to 100 milligrams. The analysis technique is based on peak intensities using the most recent values of luminous efficiency obtained from the Trailblazer measurements. The data are quite consistent with present photographic data at 1 gram, and the satellite data at 1 microgram, and tend to confirm the adopted NASA meteoroid model.

It is recognized that these observations represent only one time during the year and may be subject to seasonal variations. Such effects are the object of a current investigation.

George C. Marshall Space Flight Center
National Aeronautics and Space Administration
Marshall Space Flight Center, Alabama 35812, December 10, 1971
124-09-23-0000

REFERENCES

1. Beyer, R. R.; Green, M.; and Goetze, G. W.: Electronic and Electron Physics. Vol. 22A, Academic Press, 1966.

2. Jacchia, L. G.; Verniani, F.; and Briggs, R. E.: Smithsonian Special Report No. 175. April 23, 1965.

3. Ayers, W. G.; McCrosky, R. E.; and Shao, C. Y.: Smithsonian Special Report No. 317. June 5, 1970.

4. Cook, A. F.; Jacchia, L. G.; and McCrosky, R. E.: Smithsonian Contributions to Astrophysics. Vol. 7, 1963, pp. 209-220.

5. Dohnanyi, J. S.: Model Distribution of Photographic Meteors. Bellcomm TR-66-340-1, March 29, 1966.

6. NASA Space Vehicle Design Criteria (Environment). NASA SP-8013, March 1969.

7. Hawkins, G. S., and Upton, E. K. L.: Influx Rate of Meteors in the Earth's Atmosphere. Astrophys. J., vol. 128, 1958, pp. 727-735.

8. Clifton, K. S., and Naumann, R. J.: Pegasus Satellite Measurements of Meteoroid Penetration (February 16 – December 31, 1965). NASA TM X-1316, December 1966.

9. D'Aiutolo, C. T.; Kinard, W. H.; and Naumann, R. J.: Recent NASA Meteoroid Penetration Results from Satellites. Smithsonian Contributions to Astrophysics. Vol. 11, August 1965, pp. 239-251.

10. Naumann, R. J.: The Near-Earth Meteoroid Environment. NASA TN D-3717, November 1966.

11. Naumann, R. J.; Jex, D. W.; and Johnson, C. L.: Calibration of Pegasus and Explorer XXIII Detector Panels. NASA TR R-321, September 1969.

NASA-Langley, 1972 —— 30